

Radiative Flow with Variable Thermal Conductivity in Porous Medium

Tasawar Hayat^a, Sabir Ali Shehzad^a, Muhammad Qasim^b, and A. Alsaedi^c

^a Department of Mathematics, Quaid-i-Azam University 45320, Islamabad 44000, Pakistan

^b Department of Mathematics, Comsats Institute of Information Technology, Park Road, Chak Shehzad, Islamabad 44000, Pakistan

^c Department of Mathematics, Faculty of Science, King Abdulaziz University, P.O. Box 80257, Jeddah 21589, Saudi Arabia

Reprint requests to S. A. S.; E-mail: ali_qau70@yahoo.com

Z. Naturforsch. **67a**, 153 – 159 (2012) / DOI: 10.5560/ZNA.2012-0004

Received September 5, 2011 / revised November 27, 2011

This article considers the radiation effect on the flow of a Jeffery fluid with variable thermal conductivity. Similarity transformations are employed to convert the partial differential equations into ordinary differential equations. The resulting equations have been computed by the homotopy analysis method (HAM). The numerical values of the local Nusselt numbers are also computed. The comparison with the numerical solutions of $\theta'(0)$ is presented. The obtained results are displayed and physical aspects have been examined in detail.

Key words: Jeffery Fluid; Variable Thermal Conductivity; Non-Isothermal Stretching Surface; Porous Medium; Thermal Radiation.

1. Introduction

The boundary layer flow with heat transfer in viscous/non-Newtonian fluids is a popular area of research and a significant amount of recent research on this topic has been under taken by various authors including Ishak et al. [1], Xu and Liao [2], Sharma and Singh [3], Vyas and Srivastava [4], Abbas et al. [5], Salleh et al. [6], Hayat et al. [7], and Sahoo [8]. Such flows in porous medium have increasing applications in industries and contemporary technology. Especially the knowledge of convection in porous media is not only useful in designing the pertinent equipment but also helps in better understanding the phenomena. Few representative studies dealing with the boundary layer flows in the presence of heat transfer and porous medium have been presented in [9 – 15].

All the above mentioned studies deal with the boundary layer flow over a stretching surface with constant thermal conductivity. However it is proven now that for liquid metals the thermal conductivity varies linearly with temperature from 0 °F to 400 °F [16]. In view of such consideration, Vyas and Rai [17] reported the radiation effects on boundary layer flow of a viscous fluid with variable thermal conductivity over a non-isothermal stretching surface. But no such

attempt is presented yet for a non-Newtonian fluid. The purpose of this communication is to fill this void. Hence, the present study discusses the radiation effect on the boundary layer flow of a Jeffery fluid with variable thermal conductivity. A linear relationship between the thermal conductivity and the temperature is considered. The thermal radiation has a pivotal role in processes at high operating temperature. For instance, nuclear power plants, gas turbines, and propulsion devices for aircrafts, satellites, missiles, and space vehicles, and few examples in the engineering areas where the radiative effect is quite significant. Further, if the entire system involving the polymer extrusion process is placed in a thermally controlled environment, then the radiative effect becomes very interesting. The relevant problems for velocity and temperature are first modelled and then solved by the homotopy analysis method (HAM) [18 – 30]. The obtained solutions are plotted and analyzed.

2. Governing Equations and Analysis

Consider the flow of an incompressible Jeffery fluid over a linearly stretching sheet in a porous medium. The thermal conductivity is not constant. Two equal and opposite forces are applied along the sheet due to

which the wall is stretched keeping the position of origin unchanged. We suppose that the wall temperature $T_w(x) > T_\infty$, where T_∞ denotes the temperature of the fluid far away from the sheet. Further, both fluid and the porous medium are in local thermal equilibrium. The x - and y -axes in the Cartesian coordinate system are chosen along and normal to the sheet, respectively. The governing equations are

$$\frac{\partial u}{\partial x} + \frac{\partial v}{\partial y} = 0, \tag{1}$$

$$u \frac{\partial u}{\partial x} + v \frac{\partial u}{\partial y} = \frac{v}{1 + \lambda} \left[\frac{\partial^2 u}{\partial y^2} + \lambda_1 \left(u \frac{\partial^3 u}{\partial x \partial y^2} - \frac{\partial u}{\partial x} \frac{\partial^2 u}{\partial y^2} + \frac{\partial u}{\partial y} \frac{\partial^2 u}{\partial x \partial y} + v \frac{\partial^3 u}{\partial y^3} \right) \right] - \frac{v}{K} u, \tag{2}$$

$$\rho C_p \left[u \frac{\partial T}{\partial x} + v \frac{\partial T}{\partial y} \right] = \frac{\partial}{\partial y} \left[k \frac{\partial T}{\partial y} \right] - \frac{\partial q_r}{\partial y}, \tag{3}$$

and the subjected boundary conditions are

$$u = cx, \quad v = 0, \quad T = T_w(x) = T_\infty + Dx^\alpha \quad \text{at } y = 0, \tag{4}$$

$$u = 0, \quad T = T_\infty \quad \text{as } y \rightarrow \infty, \tag{5}$$

where u and v are the flow velocities in x - and y -directions, respectively, λ is the relaxation time, λ_1 the retardation time, ν the kinematic viscosity, K the permeability, T the temperature, k the variable thermal conductivity, ρ the density of the fluid, C_p the specific heat at constant pressure, and q_r the radiative heat flux. By making use of the Rosseland approximation (Hayat et al. [10]), the radiative heat flux q_r is given by

$$q_r = -\frac{4\sigma^*}{3k_1} \frac{\partial T^4}{\partial y}, \tag{6}$$

where σ^* is the Stefan-Boltzmann constant and k_1 the mean absorption coefficient. In view of Taylor's series, the term T^4 can be written as

$$T^4 \cong 4T_\infty^3 T - 3T_\infty^4. \tag{7}$$

By making use of (4) and (5), (3) becomes

$$\rho C_p \left[u \frac{\partial T}{\partial x} + v \frac{\partial T}{\partial y} \right] = \frac{\partial}{\partial y} \left[k \frac{\partial T}{\partial y} \right] + \frac{16\sigma T_\infty^3}{3k_1} \frac{\partial^2 T}{\partial y^2}. \tag{8}$$

The similarity transformations are defined as follows:

$$u = cx f'(\eta), \quad v = -\sqrt{c\nu} f(\eta), \quad \eta = y \sqrt{\frac{c}{\nu}}, \tag{9}$$

$$\theta(\eta) = \frac{T - T_\infty}{T_w - T_\infty},$$

where T_w is the variable wall temperature and $\theta(\eta)$ the non-dimensional form of the temperature. We consider $T = T_w(x) = T_\infty + Dx^\alpha \theta(\eta)$ at $\eta = 0$. The variable thermal conductivity is $k = k_\infty [1 + \varepsilon \theta]$ (here D and α are positive constants, k_∞ is the fluid free stream conductivity), and ε is given by

$$\varepsilon = \frac{k_w - k_\infty}{k_\infty}, \tag{10}$$

where c is a constant, k_w is the thermal conductivity at the wall, and the prime denotes differentiation with respect to η .

Equation (1) is satisfied identically, and (2)–(5) reduce to the following expressions:

$$f''' + \beta(f''^2 - ff''''') + (1 + \lambda)(ff'' - f'^2) - \frac{1}{p}(1 + \lambda)f' = 0, \tag{11}$$

$$(1 + \varepsilon \theta)\theta'' + \varepsilon \theta'^2 + \frac{4}{3}N\theta'' = \text{Pr}[\alpha \theta f' - f\theta'], \tag{12}$$

$$f(0) = 0, \quad f'(0) = 1, \quad f'(\infty) = 0,$$

$$\theta(0) = 1, \quad \text{and } \theta(\infty) = 0,$$

where $\beta = \lambda_1 c$ is the Deborah number, $p = (cK/\nu)$ is the permeability parameter, $\text{Pr} = \frac{\rho C_p \nu}{k_\infty}$ is the Prandtl number, and $N = \frac{4\sigma T_\infty^3}{Kk_\infty}$ is the radiation parameter. The local Nusselt number Nu_x is defined as

$$\text{Nu}_x = \frac{xq_w}{k(T_w - T_\infty)} \tag{13}$$

with the heat transfer q_w given by

$$q_w = -k \left(\frac{\partial T}{\partial y} \right)_{y=0}. \tag{14}$$

The dimensionless expression of (10) is

$$\text{Nu}/\text{Re}_x^{1/2} = -\theta'(0). \tag{15}$$

The problems consisting of (8) and (9) can be computed by the homotopy analysis method (HAM). For that, we express f and θ in a set of base functions

$$\{ \eta^k \exp(-n\eta) | k \geq 0, n \geq 0 \} \tag{16}$$

by

$$f(\eta) = a_{0,0}^0 + \sum_{n=0}^{\infty} \sum_{k=0}^{\infty} a_{m,n}^k \eta^k \exp(-n\eta), \tag{17}$$

$$\theta(\eta) = \sum_{n=0}^{\infty} \sum_{k=0}^{\infty} b_{m,n}^k \eta^k \exp(-n\eta) \tag{18}$$

with $a_{m,n}^k$ and $b_{m,n}^k$ as the coefficients. The initial approximations and auxiliary linear operators can be written as

$$f_0(\eta) = 1 - \exp(-\eta), \quad \theta_0(\eta) = \exp(-\eta), \quad (19)$$

$$\mathcal{L}_f = f''' - f', \quad \mathcal{L}_\theta = \theta'' - \theta, \quad (20)$$

$$\begin{aligned} \mathcal{L}_f(C_1 + C_2 e^\eta + C_3 e^{-\eta}) &= 0, \\ \mathcal{L}_\theta(C_4 e^\eta + C_5 e^{-\eta}) &= 0, \end{aligned} \quad (21)$$

where C_i ($i = 1 - 5$) are arbitrary constants.

The zeroth-order deformation problems may be expressed as

$$(1 - q)\mathcal{L}_f[\hat{f}(\eta; q) - f_0(\eta)] = qh_f\mathcal{N}_f[\hat{f}(\eta; q)], \quad (22)$$

$$(1 - q)\mathcal{L}_\theta[\hat{\theta}(\eta; q) - \theta_0(\eta)] = qh_\theta\mathcal{N}_\theta[\hat{f}(\eta; q), \hat{\theta}(\eta, q)], \quad (23)$$

$$\hat{f}(0; q) = 0, \quad \hat{f}'(0; q) = 1, \quad \hat{f}'(\infty; q) = 0, \quad (24)$$

$$\hat{\theta}(0, q) = 1, \quad \hat{\theta}'(\infty, q) = 0,$$

$$\mathcal{N}_f[\hat{f}(\eta, q)] = \frac{\partial^3 \hat{f}(\eta, q)}{\partial \eta^3} + (1 + \lambda)\hat{f}(\eta, q)$$

$$\cdot \frac{\partial^2 \hat{f}(\eta, q)}{\partial \eta^2} - (1 + \lambda) \left(\frac{\partial \hat{f}(\eta, q)}{\partial \eta} \right)^2$$

$$+ \beta \left[\left(\frac{\partial^2 \hat{f}(\eta, q)}{\partial \eta^2} \right)^2 - \hat{f}(\eta, q) \frac{\partial^4 \hat{f}(\eta, q)}{\partial \eta^4} \right]$$

$$- \frac{1}{p}(1 + \lambda) \frac{\partial \hat{f}(\eta, q)}{\partial \eta}, \quad (25)$$

$$\mathcal{N}_\theta[\hat{\theta}(\eta, q), \hat{f}(\eta, q)] = \left(1 + \frac{4}{3}N \right) \frac{\partial^2 \hat{\theta}(\eta, q)}{\partial \eta^2}$$

$$+ \varepsilon \hat{\theta}(\eta, q) \frac{\partial^2 \hat{\theta}(\eta, q)}{\partial \eta^2} + \varepsilon \left(\frac{\partial \hat{\theta}(\eta, q)}{\partial \eta} \right)^2 \quad (26)$$

$$- \text{Pr}\alpha \hat{\theta}(\eta, q) \frac{\partial \hat{f}(\eta, q)}{\partial \eta} + \text{Pr}\hat{f}(\eta, q) \frac{\partial \hat{\theta}(\eta, q)}{\partial \eta},$$

where q is the embedding parameter, h_f and h_θ are the non-zero auxiliary parameters, and \mathcal{N}_f and \mathcal{N}_θ are the nonlinear operators. For $q = 0$ and $q = 1$, one has

$$\begin{aligned} \hat{f}(\eta; 0) &= f_0(\eta), \quad \hat{\theta}(\eta, 0) = \theta_0(\eta) \text{ and} \\ \hat{f}(\eta; 1) &= f(\eta), \quad \hat{\theta}(\eta, 1) = \theta(\eta). \end{aligned} \quad (27)$$

When q increases from 0 to 1 then $f(\eta, q)$ and $\theta(\eta, q)$ varies from $f_0(\eta)$ and $\theta_0(\eta)$ to $f(\eta)$ and $\theta(\eta)$. Tay-

lor's series expansion allows the following relations:

$$f(\eta, q) = f_0(\eta) + \sum_{m=1}^{\infty} f_m(\eta)q^m, \quad (28)$$

$$\theta(\eta, q) = \theta_0(\eta) + \sum_{m=1}^{\infty} \theta_m(\eta)q^m, \quad (29)$$

$$f_m(\eta) = \frac{1}{m!} \left. \frac{\partial^m f(\eta; q)}{\partial q^m} \right|_{q=0}, \quad (30)$$

$$\theta_m(\eta) = \frac{1}{m!} \left. \frac{\partial^m \theta(\eta; q)}{\partial q^m} \right|_{q=0},$$

where the convergence of above series depends upon h_f and h_θ . Considering that h_f and h_θ are selected properly so that (22) and (23) converge at $q = 1$ and thus

$$f(\eta) = f_0(\eta) + \sum_{m=1}^{\infty} f_m(\eta), \quad (31)$$

$$\theta(\eta) = \theta_0(\eta) + \sum_{m=1}^{\infty} \theta_m(\eta). \quad (32)$$

The m th-order problems are given by

$$\mathcal{L}_f[f_m(\eta) - \chi_m f_{m-1}(\eta)] = h_f \mathcal{R}_f^m(\eta), \quad (33)$$

$$\mathcal{L}_\theta[\theta_m(\eta) - \chi_m \theta_{m-1}(\eta)] = h_\theta \mathcal{R}_\theta^m(\eta), \quad (34)$$

$$f_m(0) = f'_m(0) = f'_m(\infty) = 0, \quad (35)$$

$$\theta'_m(0) - \gamma \theta_m(0) = \theta_m(\infty) = 0, \quad (36)$$

$$\mathcal{R}_f^m(\eta) = f_{m-1}''(\eta) + (1 + \lambda)$$

$$\cdot \sum_{k=0}^{m-1} [f_{m-1-k} f_k'' - f_{m-1-k}' f_k'] + \beta \sum_{k=0}^{m-1} f_{m-1-k}'' f_k''$$

$$- \beta \sum_{k=0}^{m-1} f_{m-1-k} f_k'''' - \frac{1}{p}(1 + \lambda) f_{m-1}'(\eta),$$

$$\mathcal{R}_\theta^m(\eta) = \left(1 + \frac{4}{3}N \right) \theta_{m-1}'' + \varepsilon \sum_{k=0}^{m-1} \theta_{m-1-k} \theta_k''$$

$$+ \varepsilon \sum_{k=0}^{m-1} \theta_{m-1-k}' \theta_k' - \text{Pr}\alpha \sum_{k=0}^{m-1} \theta_{m-1-k} f_k'$$

$$+ \text{Pr} \sum_{k=0}^{m-1} \theta_{m-1-k} f_k', \quad (37)$$

$$\chi_m = \begin{cases} 0, & m \leq 1, \\ 1, & m > 1. \end{cases} \quad (38)$$

The general solutions may be written as

$$f_m(\eta) = f_m^*(\eta) + C_1 + C_2 e^\eta + C_3 e^{-\eta}, \quad (39)$$

$$\theta_m(\eta) = \theta_m^*(\eta) + C_4 e^\eta + C_5 e^{-\eta}, \quad (40)$$

where f_m^* and θ_m^* stand for the special solutions.

Table 1. Convergence of the homotopy solution for different order of approximations when $\beta = 0.1$, $\alpha = Pr = 1.0$, $N = 0.3$, $p = 2.0$, $\epsilon = \lambda = 0.2$, and $\tilde{h}_f = \tilde{h}_\theta = -0.7$.

Order of approximation	$-f''(0)$	$-\theta'(0)$
1	1.21000	0.76667
5	1.24311	0.68968
10	1.24316	0.67553
20	1.24316	0.67017
30	1.24316	0.66923
35	1.24316	0.66908
40	1.24316	0.66908
50	1.24316	0.66908

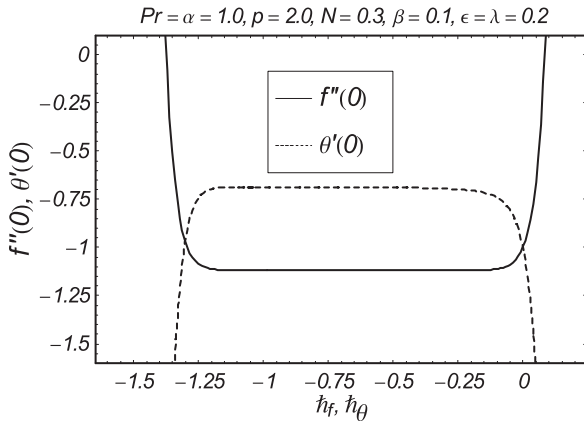


Fig. 1. \tilde{h} -curves for the functions f and θ .

3. Convergence of the Homotopy Solutions

We found that the expressions (31) and (32) have the non-zero auxiliary parameters \tilde{h}_f and \tilde{h}_θ . Such auxiliary parameters play a key role in the analysis of convergence for the obtained series solutions. In order to define the adequate values of \tilde{h}_f and \tilde{h}_θ , the \tilde{h} -curves have been portrayed for 20th-order of approximations. From Figure 1 it is noted that the range of admissible values of \tilde{h}_f and \tilde{h}_θ are $-1.2 \leq \tilde{h}_f \leq -0.1$ and $-1.1 \leq \tilde{h}_\theta \leq -0.3$. The series converges in the whole region of η when $\tilde{h}_f = \tilde{h}_\theta = -0.7$ (see Table 1).

4. Discussion

In this section, we plot Figures 2–11 for the effects of Deborah number β , permeability parameter p , ratio of relaxation time over retardation time λ , Prandtl number Pr , positive constant α , radiation parameter N , and small parameter ϵ on the velocity and temperature

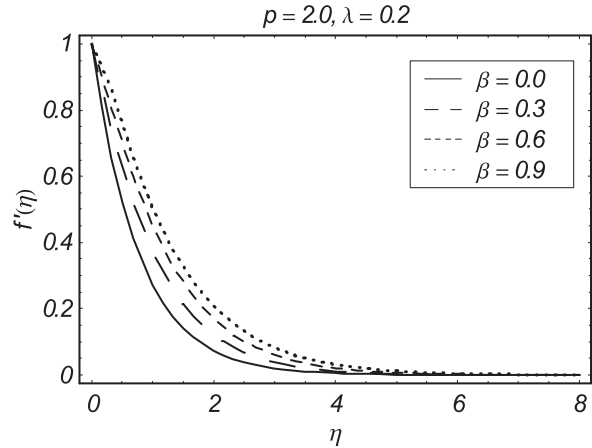


Fig. 2. Influence of β on $f'(\eta)$.

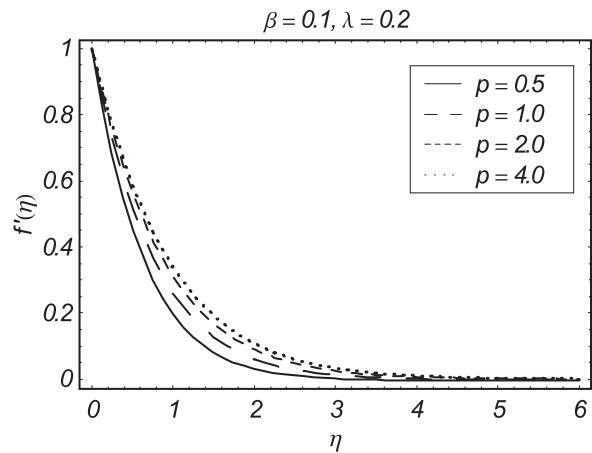


Fig. 3. Influence of p on $f'(\eta)$.

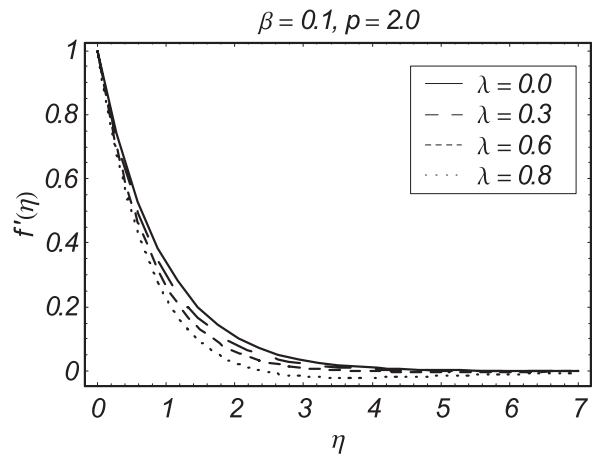


Fig. 4. Influence of λ on $f'(\eta)$.

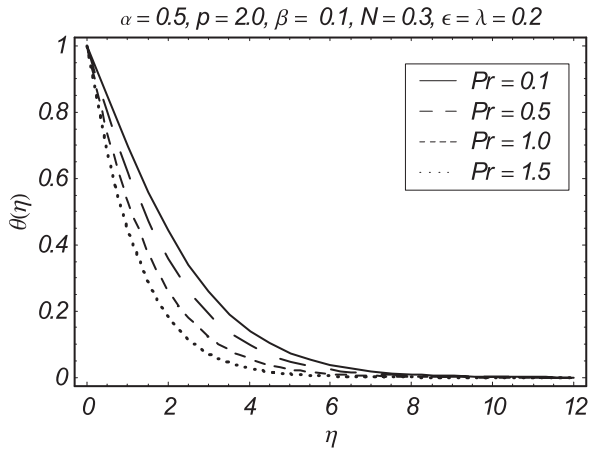


Fig. 5. Influence of Pr on $\theta(\eta)$.

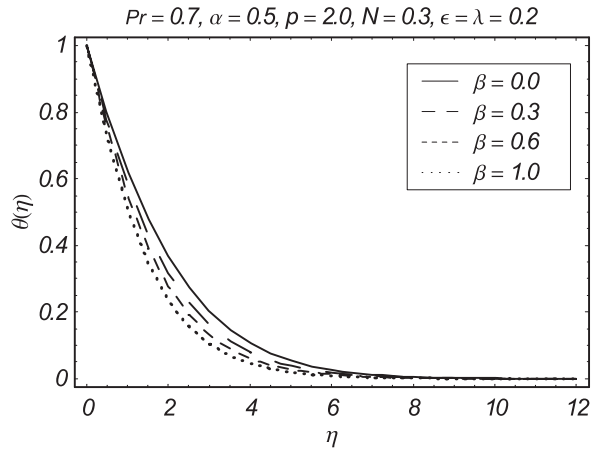


Fig. 8. Influence of β on $\theta(\eta)$.

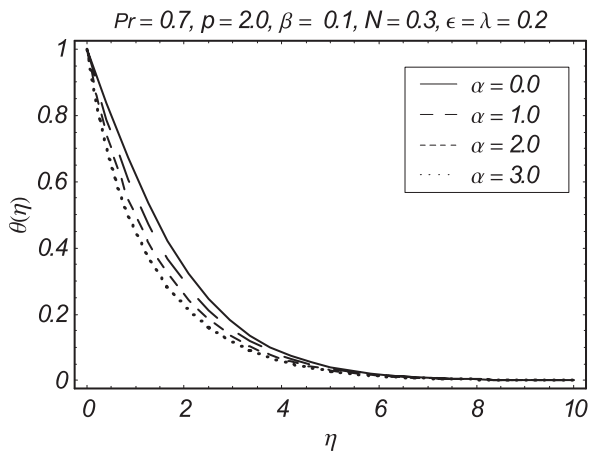


Fig. 6. Influence of α on $\theta(\eta)$.

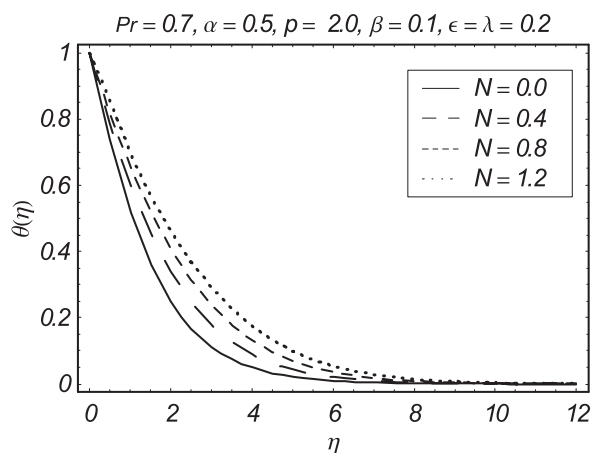


Fig. 9. Influence of N on $\theta(\eta)$.

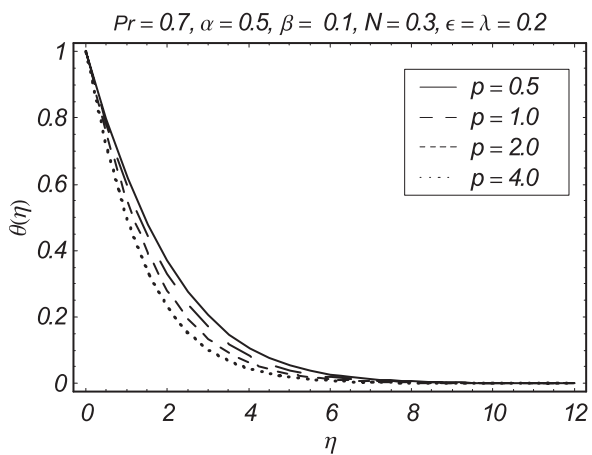


Fig. 7. Influence of p on $\theta(\eta)$.

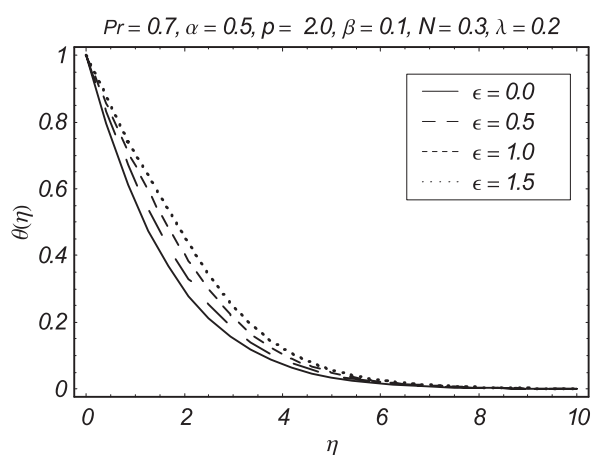


Fig. 10. Influence of ϵ on $\theta(\eta)$.

α	ε	N	p	Pr	Vyas and Rai [17]	Present results
0	0.001	1	0.5	0.023	-0.04706608006216	-0.0469873
1	0.001	1	0.5	0.023	-0.04810807780602	-0.0481857
2	0.001	1	0.5	0.023	-0.04915123655083	-0.0492375
1	0.001	1	1	0.023	-0.05813708762124	-0.0581462
1	0.001	1	2	0.023	-0.06627101076453	-0.0662179
1	0.001	2	0.5	0.023	-0.03092604001010	-0.0309465
1	0.001	3	0.5	0.023	-0.02096607234828	-0.0207548
1	0.001	5	0.5	0.023	-0.01496701292876	-0.0151473
1	0.004	1	0.5	0.023	-0.04801503596049	-0.4857646
1	0	1	0.5	0.023	-0.04814015988615	-0.0483625
1	0.001	1	0.5	0.1	-0.19563610029641	-0.1976327
1	0.001	1	0.5	0.2	-0.37208031115957	-0.3742764

Table 2. Numerical values of the local Nusselt number $\theta'(0)$ compared with the results achieved by Vyas and Rai [17].

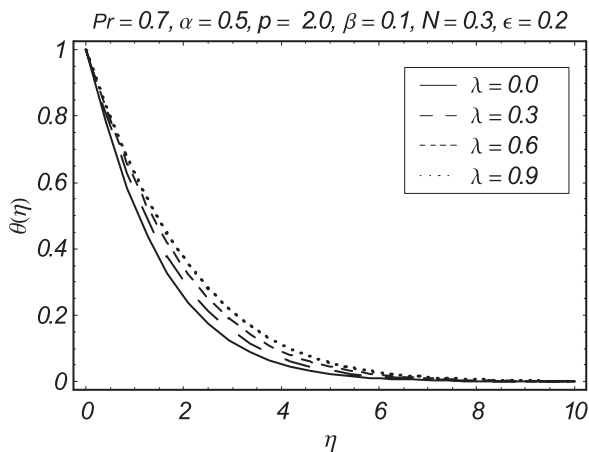


Fig. 11. Influence of λ on $\theta(\eta)$.

fields $f'(\eta)$ and $\theta(\eta)$, respectively. Figures 2–4 describe the effects of β , p , and λ on the velocity field $f'(\eta)$. Figure 2 shows that the velocity field $f'(\eta)$ decreases by increasing β . The effects of p on $f'(\eta)$ are seen in Figure 3. The velocity profile $f'(\eta)$ increases by increasing p . From Figures 2 and 3, we see that the Deborah number β and the permeability parameter p have same effects on $f'(\eta)$ in a qualitative sense. Figure 4 discloses the influence of λ on $f'(\eta)$. An increase in λ produces a decrease in velocity profile (see Fig. 4). Figures 5–11 depict the effects of different non-dimensional parameters on the temperature field $\theta(\eta)$. Figure 5 represents the effects of Pr on $\theta(\eta)$. By increasing Pr, $\theta(\eta)$ decreases. From Figure 6, we observed that the temperature field $\theta(\eta)$ decreases by increasing the values of α . Figure 7 plots the variations of p on $\theta(\eta)$. The temperature field $\theta(\eta)$ decreases when p increases. Figure 8 shows the effects of β on $\theta(\eta)$. From Figure 8, we observed that the

Table 3. Values of the local Nusselt number $-\theta'(0)$ for different values of λ , β , Pr, and p when $\alpha = 1.0$, $\varepsilon = 0.2$, and $N = 0.3$.

λ	β	Pr	p	$-\theta'(0)$
0.0	0.1	1.0	2.0	0.68704
0.3				0.66072
0.8				0.62321
1.0				0.60993
0.2	0.0			0.67584
	0.2			0.73491
	0.4			0.76583
	0.6			0.79877
		0.5		0.44584
		1.0		0.37504
		1.5		0.95721
		2.0		1.14532
			1.0	0.66931
			2.0	0.70594
			3.0	0.74092
			4.0	0.76105

temperature field $\theta(\eta)$ decreases when β increases. Figure 9 shows that the temperature profile $\theta(\eta)$ increases when N increases. Figure 10 plots the effects of ε on $\theta(\eta)$. The temperature field $\theta(\eta)$ increases when ε is increased. From Figures 9 and 10, it is obvious that N and ε have similar effects on the temperature field $\theta(\eta)$ in a qualitative sense. Figure 11 shows the effects of λ on the temperature profile. We see that $\theta(\eta)$ increases by increasing λ . By comparing Figures 4 and 11, we conclude that λ show opposite results for $f'(\eta)$ and $\theta(\eta)$.

5. Concluding Remarks

The radiative flow of a Jeffery fluid with variable thermal conductivity over a non-isothermal

stretching sheet in a porous medium is studied. The thermal conductivity varies linearly with the temperature. The key points of the present study are:

- β and λ have opposite effects on the velocity field $f'(\eta)$.
- By increasing the permeability parameter p , the velocity field $f'(\eta)$ increases.
- The temperature profile $\theta(\eta)$ decreases by increasing Pr.
- The permeability parameter has quite opposite effects on velocity and temperature profiles.
- The numerical value of the local Nusselt number decreases by increasing λ but it increases by increasing β , Pr, and p (see Tables 2 and 3).

Acknowledgement

First author thanks the support of Global Research Network for Computational Mathematics and King Saud University for this work.

- [1] A. Ishak, R. Nazar, and I. Pop, *Phys. Lett. A* **372**, 559 (2008).
- [2] H. Xu and S. J. Liao, *Comput. Math. Appl.* **57**, 1425 (2009).
- [3] P. R. Sharma and G. Singh, *J. Appl. Fluid Mech.* **2**, 13 (2009).
- [4] P. Vyas and N. Srivastava, *Appl. Math. Sci.* **4**, 2475 (2010).
- [5] Z. Abbas, Y. Wang, T. Hayat, and M. Oberlack, *Nonlin. Anal.: Real World Appl.* **11**, 3218 (2010).
- [6] M. Z. Salleh, R. Nazar, and I. Pop, *J. Taiwan Inst. Chem. E* **41**, 651 (2010).
- [7] T. Hayat, M. Qasim, and S. Mesloub, *Int. J. Numer. Meth. Fluids* **66**, 963 (2011).
- [8] B. Sahoo, *Commun. Nonlin. Sci.* **15**, 602 (2010).
- [9] R. Cortell, *Fluid Dyn. Res.* **37**, 231 (2005).
- [10] T. Hayat, Z. Abbas, I. Pop, and S. Asghar, *Int. J. Heat Mass Trans.* **53**, 466 (2010).
- [11] C. Y. Cheng, *Int. Commun. Heat Mass* **38**, 44 (2011).
- [12] P. Vyas and A. Ranjan, *Appl. Math. Sci.* **4**, 3133 (2010).
- [13] S. Mukhopadhyay, *Int. J. Heat Mass Trans.* **52**, 3261 (2009).
- [14] M. S. Abel, M. M. Nandeppanavar, and S. B. Malipatil, *Int. J. Heat Mass Trans.* **53**, 1788 (2010).
- [15] T. Hayat and Z. Abbas, *Chaos Solitons Fract.* **38**, 556 (2008).
- [16] W. M. Kay, *Convective Heat and Mass Transfer*, McGraw Hill, New York 1966.
- [17] P. Vyas and A. Rai, *Int. J. Contemp. Math. Sci.* **5**, 2685 (2010).
- [18] T. Hayat, M. Qasim, and Z. Abbas, *Z. Naturforsch.* **64a**, 231 (2010).
- [19] T. Hayat and M. Qasim, *Int. J. Heat Mass Trans.* **53**, 4780 (2010).
- [20] T. Hayat, Z. Abbas, and N. Ali, *Phys. Lett. A* **372**, 4698 (2008).
- [21] S. J. Liao, *Beyond Perturbation: Introduction to Homotopy Analysis Method*, Chapman and Hall, CRC Press, Boca Raton 2003.
- [22] S. J. Liao, *Stud. Appl. Math.* **117**, 2529 (2006).
- [23] S. J. Liao, *Appl. Math. Comput.* **147**, 499 (2004).
- [24] A. S. Bataineh, M. S. M. Noorani, and I. Hashim, *Commun. Nonlin. Sci.* **14**, 409 (2009).
- [25] S. Abbasbandy, *Z. Angew. Math. Phys.* **59**, 51 (2008).
- [26] T. Hayat, S. A. Shehzad, and M. Qasim, *Int. J. Numer. Meth. Fluids* **67**, 1418 (2011).
- [27] T. Hayat, S. A. Shehzad, M. Qasim, and S. Obaidat, *Nucl. Eng. Des.*, **243**, 15 (2012).
- [28] T. Hayat, S. A. Shehzad, A. Rafique, and M. Y. Malik, *Int. J. Numer. Meth. Fluids* doi:10.1002/fld.2515.
- [29] I. Hashim, O. Abdulaziz, and S. Momani, *Commun. Nonlin. Sci.* **14**, 674 (2009).
- [30] T. Hayat, Z. Abbas, M. Sajid, *Chaos Solitons Fract.* **39**, 840 (2009).